PHYSICS AND CHEMISTRY OF SOLID STATE
V. 26, No. 3 (2025) pp. 699-704
Section: Physics

DOI: 10.15330/pcss.26.3.699-704

Vasyl Stefanyk Carpathian National University

ФІЗИКА І ХІМІЯ ТВЕРДОГО ТІЛА
Т. 26, № 3 (2025) С. 699-704
Фізико-математичні науки

PACS: 61.05.C-, 68.55.ag , 77.55.hf

ISSN 1729-4428 (Print)
ISSN 2309-8589 (Online)

A.S. Revenko[1], V.V. Kidalov[2,3], O.I. Gudymenko[4]

Structural properties of ZnO films obtained on SiC/porous-Si by the method of high frequence magnetron sputtering

[1]University College Dublin, Belfield, Dublin 4, Ireland, andriy.revenko@ucd.ie,
[2]Technical University Dortmund, Experimentelle Physik 2, August-Schmidt-Straße 1, Germany,
[3]Dmytro Motornyi Tavria State Agrotechnological University, Melitopol, Ukraine,
[4]V.E. Lashkaryov Institute of Semiconductor Physics NAS of Ukraine, Kyiv, Ukraine,

The morphological and structural properties of ZnO thin films grown by RF magnetron sputtering using a SiC/porous-Si/Si template were studied. The preparation of the ZnO/SiC/porous-Si/Si heterostructure was carried out in two stages: deposition of SiC films by solid-phase epitaxy followed by the deposition of ZnO films by radio frequency magnetron sputtering.

SiC buffer layers on the porous silicon substrate allow for the growth of ZnO films with low residual mechanical stress, measured at -82.3 MPa. A comparative analysis with data from other studies indicates the relatively high quality of the obtained structures.

Keywords: zinc oxide (ZnO), silicon carbide (SiC), porous silicon (por-Si), scanning electron microscopy (SEM), X-ray diffraction (XRD).

Received 08 June 2025; Accepted 26 September 2025.

Introduction

Zinc oxide, particularly in the form of thin films and nanostructures, is widely used in optoelectronic devices as a luminescent material, sensitive layers for gas and biological sensors, catalysts, and detectors of ultraviolet, X-ray, and gamma radiation [1–6]. The structure, morphology, and properties of zinc oxide significantly depend on its synthesis conditions and fabrication technology.

Various methods exist for the synthesis of ZnO films, including chemical vapor deposition, pulsed laser deposition, vacuum arc deposition, hydrothermal synthesis, and molecular beam epitaxy [7–11]. However, most of these methods are costly, making it relevant to investigate more economical and accessible technologies for ZnO film fabrication. At the same time, RF magnetron sputtering is a relatively inexpensive method for obtaining high-quality ZnO films [1,12–15].

Silicon and sapphire are the most common substrates for the epitaxial growth of ZnO films [16–19]. However, sapphire, being a dielectric, significantly reduces the quality of electronic devices based on ZnO/Al_2O_3 structures. The ZnO/Si structure provides a more efficient platform for electronic devices. However, the poor lattice matching and thermal expansion coefficients between ZnO and Si complicate the growth of epitaxial ZnO thin films directly on Si. In a previous study, we demonstrated that using a porous silicon substrate reduced elastic deformation in ZnO films, but the strain value was still high at 1.025 GPa (tensile strain) [13]. Additionally, silicon substrates are unstable under high growth temperatures and oxygen-rich environments, which can lead to surface oxidation. To address these issues, it is recommended to use buffer layers, such as silicon carbide (SiC) [20,21].

The aim of this study is to further develop the methodology of RF magnetron sputtering combined with SiC/porous-Si/Si structures, which appears to be a promising approach for obtaining high-quality ZnO films. This study investigates the morphological and structural properties of ZnO films obtained by RF magnetron

sputtering on SiC/porous-Si/Si substrates and presents the comparative analysis of the residual stresses in the ZnO films with those reported in other studies.

I. Research methods

The preparation of the ZnO/SiC/porous-Si/Si heterostructure was conducted in the following stages:

- Deposition of SiC film on porous Si using solid-phase epitaxy.
- Deposition of ZnO films by RF magnetron sputtering.

The resulting structures were analyzed using scanning electron microscopy (SEM) and X-ray diffraction (XRD). SEM studies were performed using Tescan Mira 3 LMU and Zeiss Supra 25 microscopes, and XRD was conducted using a Philips X'Pert PRO - MRD diffractometer with Cu Kα radiation (wavelength λ= 0.15406 nm). The anode voltage was 45 kV, and the current was 40 mA.

II. Results and discussion

The porous silicon substrate was sourced from Smart Membranes GmbH (Germany). The pore depth and diameter are 2000 nm and 15 nm, respectively, with a wafer diameter of 2 inches (Fig. 1).

To deposit the SiC buffer layer, the silicon substrate with a porous surface was treated in an atmosphere of CO and SiH_4 gases. The SEM images of the SiC films on the porous Si substrate (cross-section) are presented in Fig. 2. The porous Si/Si sample was heated using a graphite heater to a temperature of 1000 °C. A HORIBA gas regulator was used to control the flow of CO and SiH4 gases, with a total gas mixture pressure of 133 Pa and flow rates of 14 cm³/min and 3.5 cm³/min, respectively. The synthesis process lasted for 20 minutes.

We utilized the porous surface of silicon to increase the effective surface area and, thereby, enhance the intensity of the SiC layer formation process. The principal chemical reaction for this process is as follows:

2Si(solid) + CO (gas) = SiC (solid) + SiO↑(gas)

During annealing, carbon monoxide penetrates the depth of the porous surface layers of the silicon substrate. Simultaneously, silicon atoms are replaced by carbon atoms within the mesoporous silicon columns, forming SiC molecules and creating silicon vacancies. As a result, the mesoporous silicon surface layer is transformed into a silicon carbide film. Beneath this newly formed SiC layer, silicon vacancies coalesce to form pores. The detailed mechanism of the transformation from mesoporous silicon layers into silicon carbide films, as well as the formation of macroporous silicon between the SiC layer and the single-crystalline silicon substrate, is described in more detail in reference [22].

Following magnetron sputtering, the surface of the SiC/porous-Si substrate was covered with a ZnO film (Fig. 3). The technological parameters for ZnO film deposition were as follows: processing time 600 seconds, substrate temperature 300 °C, residual pressure 10^{-3} Pa, argon and oxygen pressures 1 Pa and 0.1 Pa, respectively, and RF magnetron discharge power 200 W. The resulting ZnO film exhibits a columnar structure.

The X-ray diffraction (XRD) pattern of the ZnO films is shown in Fig. 4. A diffraction peak is observed at 34.40°, with a full width at half maximum (FWHM) of 0.582°. The presence of a triplet in the range of 31°–36° indicates the formation of a polycrystalline hexagonal ZnO phase [23].

X-ray diffraction (XRD) measurements reveal that the ZnO films exhibit a nanocrystalline structure. The average crystallite size D was calculated using the width of the (002) peak and Scherrer's formula:

$$D = \frac{b \cdot \lambda}{\beta \cdot \cos(\theta)} \quad (1)$$

where b is a correction factor 0.9, λ is the wavelength of X-ray radiation (λ=0.15418 nm), β is the full width at half maximum (FWHM) of the (002) peak in radians, and θ is the diffraction angle [24–27]. The calculated average crystallite size is 15 nm.

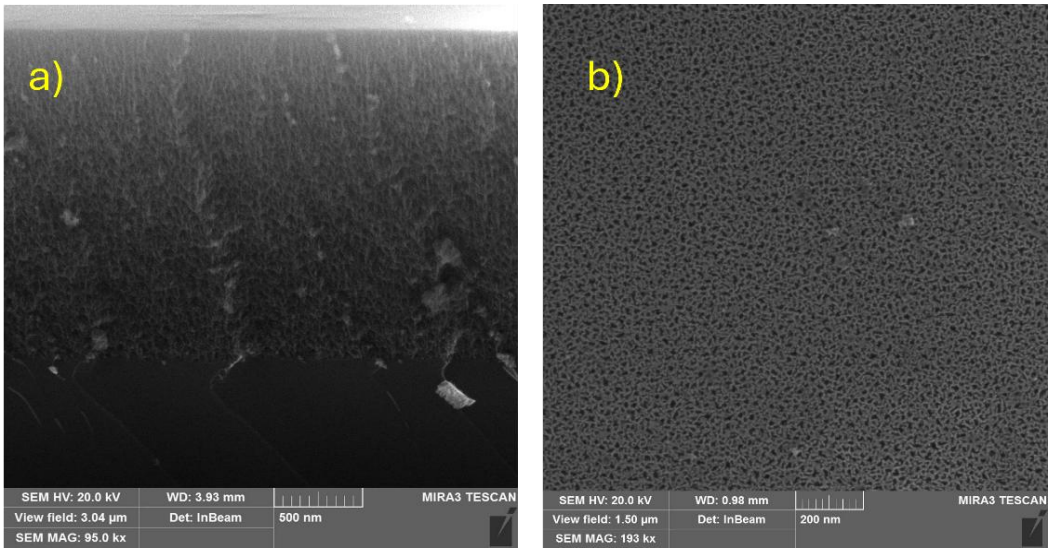

Fig. 1. SEM images of the cross-sections a) and surface b) of porous Si/Si .

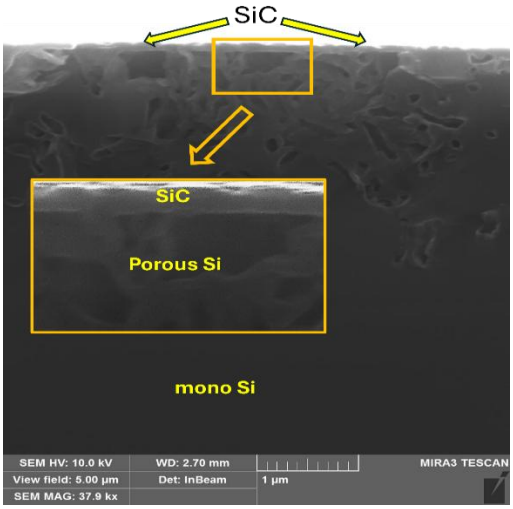

Fig. 2. SEM image of cross-section of SiC layer synthesized on the porous Si.

In our previous work on ZnO/por-Si samples, the crystallite sizes were in the range of 100–200 nm. We hypothesize that SiC buffer layer led to a reduction in the crystallite sizes in the ZnO films and, ultimately, as discussed below, to a significant decrease in the mechanical stresses [13].

The residual stress in the ZnO film was calculated using the following equation [28]:

$$\sigma = -233 \times \frac{(c_{exp} - c_{free})}{c_{free}} \quad (2)$$

where c_{exp} is the lattice parameter of the c-axis in the ZnO film and c_{free} is the lattice parameter of stress-free ZnO (bulk or powder). The value of c_{exp} was calculated from XRD measurements according to Bragg's equation:

$$d_{hkl} \cdot 2\sin(\theta) = \lambda \quad (3)$$

where d_{hkl} is the lattice spacing, λ is the wavelength of CuKα radiation (0.15406 nm), and θ is the Bragg angle (half of the 2θ value). Given that ZnO film has a wurtzite hexagonal structure, the following formula can also be applied [29]:

$$\frac{1}{d_{hkl}^2} = \frac{4}{3}\left(\frac{h^2+hk+k^2}{a^2}\right) + \frac{l^2}{c^2} \quad (4)$$

where a and c are the lattice constants. Using Eq. (3) and Eq. (4), we calculated a value of 0.5208 nm for the c_{exp} parameter. The lattice constant for strain-free ZnO is 0.5206 nm (JCPDS #36-1451 data card).

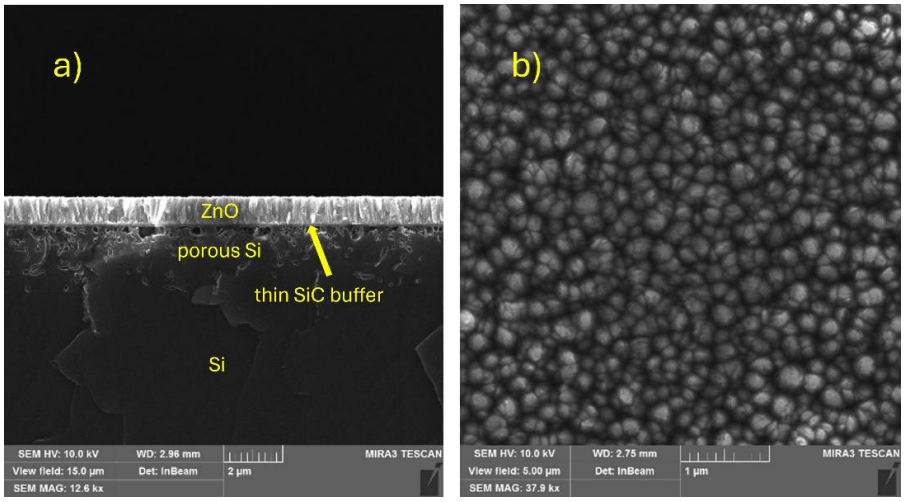

Fig. 3. SEM image of the cross-section a) and surface b) of the ZnO/porous-Si/Si heterostructure.

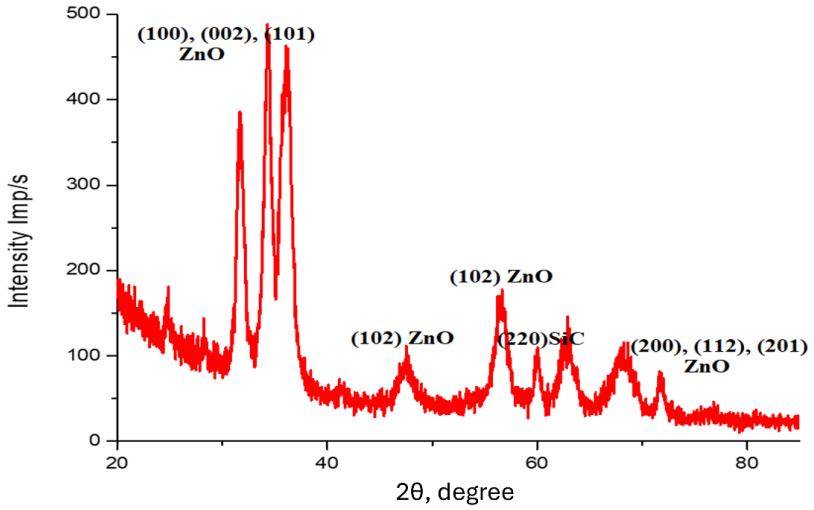

Fig. 4. X-ray diffraction pattern of ZnO/SiC/porous-Si/Si samples.

Thus, using the formula (4) the calculated value for the residual stress is -82.3 MPa, indicating compressive biaxial stress.

The residual stress value of −82.3 MPa-82.3 is significantly lower than the stress value of 1.207 GPa observed in our earlier study for ZnO/porous-Si structures without the SiC buffer layer[13].

Moreover, the stress values obtained in this study are comparable to or lower than those reported in other studies. For example, stress values for ZnO films on Si substrates (using the MBE method) ranged from 0.2–0.4 GPa for porous Si structures and 0.9–1 GPa for single-crystalline Si structures [30]. Similarly, for ZnO films on Si obtained using RF magnetron sputtering, stress values ranged from 0.48 to 0.31 GPa [14]. Comparatively, ZnO/Al_2O_3 structures grown using MBE methods can exhibit much higher stress values, reaching 3.306 GPa [11].

Conclusions

This paper presents the results of studying ZnO/SiC/porous-Si/Si heterostructures obtained through two stages: the deposition of SiC films by solid-phase epitaxy, followed by the deposition of ZnO films by magnetron sputtering. The resulting heterostructures were analyzed using scanning electron microscopy and X-ray diffraction.

Based on the XRD patterns, the presence of a polycrystalline hexagonal ZnO phase was confirmed with the residual stress of −82.3 being significantly lower than in our previous work on ZnO/porous-Si structures. Moreover, the residual stresses in the ZnO films are much lower than those reported in the literature for ZnO films on Si and Al_2O_3 substrates.

Thus, it can be concluded that the cost-effective RF magnetron sputtering method in combination with a SiC buffer layer on porous silicon allows the production of ZnO films with high structural quality. This methodology holds promise for further research and optimization.

Acknowledgments

The research was supported by Science Foundation Ireland under the Supplemental Grant for Displaced Researchers scheme (SFI 20/FFP-P/8728 (S)) and by the German Research Foundation under the Walter Benjamin Programme (KI 2865/1-1, DFG project number 529795573).

Revenko A.S. – Scientific Researcher, PhD;
Kidalov V.V. – Professor;
Gudymenko O.I. – Senior Research Fellow, PhD.

[1] M. Aleksanyan, A. Sayunts, G. Shahkhatuni, Z. Simonyan, G. Shahnazaryan, V. Aroutiounian, *Gas Sensor Based on ZnO Nanostructured Film for the Detection of Ethanol Vapor*, Chemosensors, 10(7), 245 (2022); https://doi.org/10.3390/chemosensors10070245.

[2] B. Li, F. Zhang, W. Liu, X. Chen, Y. Gao, F. Wang, X. Zhang, X. Yan, T. Cheng, *An Ultraviolet Sensor Based on Surface Plasmon Resonance in No-Core Optical Fiber Deposited by Ag and ZnO Film*, Surface and Interfaces, 31, 102074 (2022); https://doi.org/10.1016/j.surfin.2022.102074.

[3] S. Nasirian, F. Hadizadeh, Polymer, *A Cheap Self-Powered UV-Photodetector Based on Layer-by-Layer Arrangement of Polyaniline and ZnO*, 245, 124699 (2022); https://doi.org/10.1016/j.polymer.2022.124699.

[4] R. Wahab, N. Ahmad, M. Alam, J. Ahmad, *Nanorods of ZnO: An Effective Hydrazine Sensor and Their Chemical Properties*, Vacuum, 164, 290(2019); https://doi.org/10.1016/j.vacuum.2019.04.036.

[5] A.M. Ali, F.A. Harraz, A.A. Ismail, S.A. Al-Sayari, H. Algarni, A.G. Al-Sehemi, *Synthesis of Amorphous ZnO–SiO2 Nanocomposite with Enhanced Chemical Sensing Properties*, Thin Solid Films, 605, 277 (2016); https://doi.org/10.1016/j.tsf.2015.11.044.

[6] B.-R. Wang, R.-Z. Wang, Y.-J. Bai, L.-Y. Liu, Q.-L. Jiang, *Zinc Oxide Nanonets with Hierarchical Crystalline Nodes: High-Performance Ethanol Sensors Enhanced by Grain Boundaries*, Journal of Alloys and Compounds, 877, 160277 (2021); https://doi.org/10.1016/j.jallcom.2021.160277.

[7] J.-J. Wu, S.-C. Liu, *Catalyst-Free Growth and Characterization of ZnO Nanorods*, Journal of Physical Chemistry B, 106(37), 9546 (2002); https://doi.org/10.1021/jp025969j.

[8] H. Takikawa, K. Kimura, R. Miyano, T. Sakakibara, *ZnO Film Formation Using a Steered and Shielded Reactive Vacuum Arc Deposition*, Thin Solid Films, 377–378, 74 (2000); https://doi.org/10.1016/S0040-6090(00)01387-0.

[9] A. Fouchet, W. Prellier, B. Mercey, L. Méchin, V.N. Kulkarni, T. Venkatesan, *Investigation of Laser-Ablated ZnO Thin Films Grown with Zn Metal Target: A Structural Study*, Journal of Applied Physics, 96(6), 3228 (2004); https://doi.org/10.1063/1.1772891.

[10] H. Hu, X. Huang, C. Deng, X. Chen, Y. Qian, *Hydrothermal Synthesis of ZnO Nanowires and Nanobelts on a Large Scale*, Materials Chemistry and Physics, 106(1), 58 (2007); https://doi.org/10.1016/j.matchemphys.2007.05.016.

[11] S.-Y. Ting, P.-J. Chen, H.-C. Wang, C.-H. Liao, W.-M. Chang, Y.-P. Hsieh, C.C. Yang, *Crystallinity Improvement of ZnO Thin Film on Different Buffer Layers Grown by MBE*, Journal of Nanomaterials, 2012, 929278 (2012); https://doi.org/10.1155/2012/929278.

[12] Q.P. Wang, D.H. Zhang, Z.Y. Xue, X.T. Hao, *Violet Luminescence Emitted from ZnO Films Deposited on Si Substrate by Rf Magnetron Sputtering*, Applied Surface Science, 201(1), 123 (2002); https://doi.org/10.1016/S0169-4332(02)00570-6.

[13] V. Kidalov, A. Dyadenchuk, Y. Bacherikov, A. Zhuk, T. Gorbanuk, I. Rogozin, *Structural and Optical Properties of ZnO Films Obtained on Mesoporous Si Substrates by the Method of HF Magnetron Sputtering*, Turkish Journal of Physics, 44(1), 57 (2020); https://doi.org/10.3906/fiz-1909-10.

[14] I. Ozen, M.A. Gülgün, *Residual Stress Relaxation and Microstructure in ZnO Thin Films*, Advances in Science and Technology, 45, 1316 (2006); https://doi.org/10.4028/www.scientific.net/AST.45.1316.

[15] Z.D. Sha, J. Wang, Z.C. Chen, A.J. Chen, Z.Y. Zhou, X.M. Wu, L.J. Zhuge, *Initial Study on the Structure and Optical Properties of ZnO Film on Si(111) Substrate with a SiC Buffer Layer*, Physica E: Low-dimensional Systems and Nanostructures, 33(1), 263 (2006); https://doi.org/10.1016/j.physe.2006.03.138.

[16] Ü. Akın, A. Houimi, B. Gezgin, Y. Gündoğdu, S. Kılıç, B. Mercimek, A. Berber, S.Y. Gezgin, *The Electrical Properties of ZnO/Si Heterojunction Diode Depending on Thin Film Thickness*, Journal of the Korean Physical Society, 81(2), 139 (2022); https://doi.org/10.1007/s40042-022-00499-7.

[17] M.P. Gönüllü, D.D. Çakıl, C. Çetinkaya, *The Attitude of ZnO/Al2O3 Film Produced by Ultrasonic Spray Pyrolysis Under Thermal Annealing*, Gazi University Journal of Science - Part C: Design and Technology, 10(4), 1026 (2022); https://doi.org/10.29109/gujsc.1137863.

[18] H.-J. Ko, T. Yao, Y. Chen, S.-K. Hong, *Investigation of ZnO Epilayers Grown under Various Zn/O Ratios by Plasma-Assisted Molecular-Beam Epitaxy*, Journal of Applied Physics, 92(8), 4354 (2002); https://doi.org/10.1063/1.1509103.

[19] Y. Zhang, G. Du, B. Zhang, Y. Cui, H. Zhu, Y. Chang, *Properties of ZnO Thin Films Grown on Si Substrates by MOCVD and ZnO/Si Heterojunctions*, Semiconductor Science and Technology, 20(11), 1132 (2005); https://doi.org/10.1088/0268-1242/20/11/006.

[20] X. Xiaopeng, C. Xiaoqing, S. Lijie, M. Shun, F. Zhuxi, *Photoelectric Conversion Characteristics of ZnO/SiC/Si Heterojunctions*, Journal of Semiconductors, 31(10), 103002 (2010); https://doi.org/10.1088/1674-4926/31/10/103002.

[21] V. Kidalov, A. Dyadenchuk, C. Abbasova, V. Baturin, O. Karpenko, O. Gudimenko, *2022 IEEE 12th International Conference Nanomaterials: Applications & Properties (NAP)*, *Synthesis and Characterization of SiC-Based Thin Film Heterostructures*, IEEE, 2022, pp. 01 https://doi.org/10.1109/NAP55339.2022.9934602.

[22] V.V. Kidalov, A.S. Revenko, D. Duleba, R.A. Redko, *Synthesis, Properties, and Application of Nanostructured ZnO Materials*, ECS Journal of Solid State Science and Technology, 13(11), 114003 (2024); https://doi.org/10.1149/2162-8777/ad89f8.

[23] C.J. Raj, R.K. Joshi, K.B.R. Varma, *Synthesis from Zinc Oxalate, Growth Mechanism and Optical Properties of ZnO Nano/Micro Structures*, Crystal Research and Technology, 46(11), 1181 (2011); https://doi.org/10.1002/crat.201100201.

[24] E.F. Kaelble, *Handbook of X-Rays: For Diffraction, Emission, Absorption, and Microscopy* (McGraw-Hill, New York, 1967).

[25] A. Khorsand Zak, W.H. Abd. Majid, M.E. Abrishami, R. Yousefi, *X-Ray Analysis of ZnO Nanoparticles by Williamson–Hall and Size–Strain Plot Methods*, Solid State Sciences, 13(1), 251 (2011); https://doi.org/10.1016/j.solidstatesciences.2010.11.024.

[26] A. Singh, H.L. Vishwakarma, *Study of Structural, Morphological, Optical and Electroluminescent Properties of Undoped ZnO Nanorods Grown by a Simple Chemical Precipitation*, Materials Science-Poland, 33, 751 (2015); https://doi.org/10.1515/msp-2015-0112.

[27] S.A. Studenikin, N. Golego, M. Cocivera, *Fabrication of Green and Orange Photoluminescent, Undoped ZnO Films Using Spray Pyrolysis*, Journal of Applied Physics, 84(4), 2287 (1998); https://doi.org/10.1063/1.368295.

[28] D. Dimova-Malinovska, H. Nichev, O. Angelov, *Correlation between the Stress in ZnO Thin Films and the Urbach Band Tail Width*, Physica Status Solidi C, 5(10), 3353 (2008); https://doi.org/10.1002/pssc.200778886.

[29] M. Mazhdi, P. Hossein Khani, *Structural Characterization of ZnO and ZnO Nanoparticles Prepared by Reverse Micelle Method*, International Journal of Nano Dimensions, 2(4), 233 (2012); https://doi.org/10.7508/ijnd.2011.04.004.

[30] M.S. Kim, K.G. Yim, J.-Y. Leem, S. Kim, G. Nam, D.-Y. Lee, J.S. Kim, J.S. Kim, *Thickness Dependence of Properties of ZnO Thin Films on Porous Silicon Grown by Plasma-Assisted Molecular Beam Epitaxy*, Journal of the Korean Physical Society, 59(3), 2354 (2011); https://doi.org/10.3938/jkps.59.2354.

А.С. Ревенко[1], В.В. Кідалов[2,3], О.Й. Гудименко[4]

Структурні властивості плівок ZnO, отриманих на SiC/поруватому Si методом високочастотного магнетронного розпилення

[1]Університетський коледж Дубліна, Белфілд, Дублін 4, Ірландія, andriy.revenko@ucd.ie;
[2]Технічний університет Дортмунда, Експериментальна фізика 2, Німеччина;
[3]Таврійський державний агротехнологічний університет імені Дмитра Моторного, Мелітополь, Україна;
[4]Інститут фізики напівпровідників ім. В.Є. Лашкарьова НАН України, Київ, Україна

Досліджено морфологічні та структурні властивості тонких плівок ZnO, вирощених методом високочастотного магнетронного розпилення з використанням підкладки SiC/поруватий Si/Si. Гетероструктуру ZnO/SiC/поруватий Si/Si сформовано у два етапи: осадження плівок SiC методом твердофазної епітаксії та нанесення плівок ZnO методом високочастотного магнетронного розпилення.

Буферні шари SiC на підкладці з пористого кремнію забезпечують формування плівок ZnO з низькими залишковими механічними напруженнями (–82,3 МПа). Порівняльний аналіз із літературними даними свідчить про відносно високу якість отриманих структур.

Ключові слова: оксид цинку (ZnO), карбід кремнію (SiC), поруватий кремній (por-Si), скануюча електронна мікроскопія (SEM), рентгенівська дифракція (XRD).